PERGAMON

Computers and Structures 75 (2000) 321–334

Computers & Structures

www.elsevier.com/locate/compstruc

A unified approach for shear-locking-free triangular and rectangular shell finite elements

Kai-Uwe Bletzinger[a,*], Manfred Bischoff[b], Ekkehard Ramm[b]

[a]*Institute of Structural Analysis, University of Karlsruhe Kaiserstr 12, 76131, Karlsruhe, Germany*
[b]*Institute of Structural Mechanics, University of Stuttgart, 70550 Stuttgart, Germany*

Abstract

A new concept for the construction of locking-free finite elements for bending of shear deformable plates and shells, called DSG (Discrete Shear Gap) method, is presented. The method is based on a pure displacement formulation and utilizes only the usual displacement and rotational degrees of freedom (dof) at the nodes, without additional internal parameters, bubble modes, edge rotations or whatever. One unique rule is derived which can be applied to both triangular and rectangular elements of arbitrary polynomial order. Due to the nature of the method, the order of numerical integration can be reduced, thus the elements are actually cheaper than displacement elements with respect to computation time. The resulting triangular elements prove to perform particularly well in comparison with existing elements. The rectangular elements have a certain relation to the Assumed Natural Strain (ANS) or MITC-elements, in the case of a bilinear interpolation, they are even identical.

Keywords: Finite element; Reissner/Mindlin shells and plates; Triangular and rectangular; Shear-locking; ANS; Linear elastic

1. Introduction

The development of efficient shear deformable plate and shell elements of the Reissner–Mindlin type has a more than 30 year old history and it is completely impossible to give an overview over the innumerable concepts, invented by both mathematicians and engineers in the past. Therefore, the method described in the present paper is solely compared to those concepts that are either the most efficient in the experience of the authors, or have some similarity to the method itself. Plate and shell formulations of the Kirchhoff–Love type, without consideration of transverse shear effects, are not addressed in the present study.

Regarding the multitude of different concepts, it can be recognized that most element developers concentrate their efforts either on triangular elements or on quadrilaterals. There are only few papers, where a successful concept for quadrilaterals is transferred to triangles or vice versa.

It is also apparent, that the problem of transverse shear locking is practically solved for structured meshes with regular element shapes. Here, most of the elements described in the past 25 years perform well. However, in the case of distorted meshes (e.g. for a

* Corresponding author. Tel.: +49-721-608-2283; fax: +49-721-608-6015.

E-mail addresses: kub@bau-verm.uni-karlsruhe.de (K.-U. Bletzinger), bischoff@statik.uni-stuttgart.de (M. Bischoff), eramm@statik.uni-stuttgart.de (E. Ramm).

0045-7949/00/$ - see front matter
PII: S0045-7949(99)00140-6

complex geometry or when automatic meshers within adaptivity are used) there are still some problems.

The question, whether triangles or quadrilaterals are the 'better' choice, still seems to be not yet decided. While most of the quadrilaterals exhibit better performance concerning convergence rates, triangles are definitely easier to apply for free-meshing algorithms, and therefore, preferred in adaptivity.

For triangular elements it is remarkable that many formulations contain awkward procedures while deriving the element stiffness matrix. Especially, when additional dof are introduced (e.g. rotations at the midpoints of the edges, bubble modes, etc.) and condensed out later on to preserve the global number of dof, the question arises, if a similar result could be obtained by simpler procedures.

In the present paper, a methodology is described which allows the formulation of efficient finite elements of arbitrary polynomial order, either triangular or rectangular, with one unique, simple rule. The method is based on the explicit satisfaction of the kinematic equation for the shear strains at discrete points and effectively eliminates the parasitic shear strains. The essential step is the calculation of discrete shear gaps (DSG) at the nodes and their interpolation across the element domain, thus obtaining a shear strain distribution which is free of parasitic parts.

The concept could be regarded as a B-bar method, because only the differential operator for the strain-displacement relation is affected. The formulation uses the standard dof of pure displacement elements and does not introduce extra nodes or internal parameters. The only modification with respect to displacement elements is the different calculation of transverse shear strains. This, in turn, makes it most easy to implement the element into an existing code.

The resulting elements are free of locking, pass the patch-test, and show reduced sensitivity to mesh distortions. The computation time for the construction of the element stiffness matrix is less than for pure displacement elements, which makes the method extremely efficient.

The most apparent similarities to the present method can be observed in the so-called Kirchhoff mode (KM) concept, originally proposed by Hughes and Tezduyar [16] (see Hughes and Taylor [15] for a corresponding linear triangle). Here, conditions for the shear strains are formulated along the edges of the element and the resulting discrete shear strains at the nodes are interpolated over the element domain with the standard shape functions.

Although initially not realized, the so-called ANS (Assumed Natural Strain) or MITC (Mixed Interpolation of Tensorial Components) approach of Bathe and co-workers [4,8] leads to identical elements as the KM concept in the case of a bilinear interpolation. The method is based on interpolation of the shear strains from particularly chosen sampling points and successfully eliminates their parasitic part. Until today, the MITC4 element is probably the most efficient bilinear element for the analysis of both thick and thin plates and shells. Recent developments concern the reduction of distortion sensitivity of the MITC4 element through stabilization methods [17].

It seems, however, that the transfer of both the KM and the ANS concept to triangles is not trivial. Especially a proper choice of feasible sampling points in the ANS formulation proves to be more problematic than for rectangles. One of the first successful linear triangular elements has been developed by Xu [27] on the basis of the KM concept, introducing additional dof in the element center ('bubble modes').

Although the method presented in this study could be classified as an ANS method, from the point of view of the authors, there are some advantages. Due to the fact that the element formulation evolves in a natural way for any kind of element, regardless of shape and polynomial order, there is no need to choose an interpolation for the shear strains or to specify any sampling points. In the case of rectangles, the present concept leads to the same stiffness matrices as the KM or ANS elements, respectively. For triangles, no equivalent could be found in the literature. This leads us to the opinion that the present DSG-elements might be the missing link between rectangular and triangular KM or ANS elements.

Due to the multitude of different concepts to eliminate shear locking in beams, plates and shells this short review is necessarily incomplete. To sum up, one can say, that the basic idea of the DSG concept appears in the literature in numerous different shapes. The main contribution of the present paper is the systematic development of a class of efficient elements by straightforward realization of the basic concept, described in Section 2.

2. The basic idea

The basic idea is most simply explained with the example of the Timoshenko beam theory. The deformation of the beam continuum is described by the displacement $v(x)$ of the beam center line and rotation $\beta(x)$ of the cross section, Fig. 1. The difference of rotation $\beta(x)$ and the gradient of the displacement $v'(x)$ defines the shear deformation $\gamma(x)$ at any point x along the beam:

$$\gamma(x) = v'(x) + \beta(x) \tag{1}$$

The special case of pure bending is reflected by the so-called Bernoulli condition (Kirchhoff for plates), i.e.

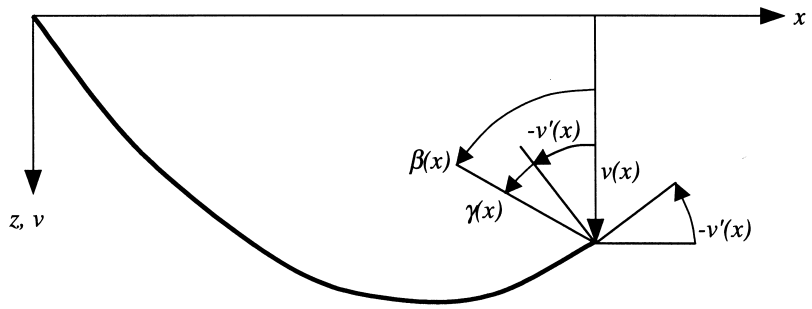

Fig. 1. Timoshenko beam.

$$\gamma(x) = v'(x) + \beta(x)$$

that the shear deformation has to vanish:

$$0 \equiv v'(x) + \beta(x) \tag{2}$$

The total displacement of the beam is due to deformation with respect to bending and shear. The shear related part is determined by integration of (1):

$$\Delta v_\gamma(\hat{x}) = \int_{x_0}^{\hat{x}} \gamma \, \mathrm{d}x = v|_{x_0}^{\hat{x}} + \int_{x_0}^{\hat{x}} \beta \, \mathrm{d}x$$
$$= \underbrace{v(\hat{x}) - v(x_0)}_{\Delta v} + \Delta v_b \tag{3}$$

which describes the increase of displacement due to shear between the positions x_0 and $\hat{x}$. Δv_γ can be identified as the 'shear gap', the difference between the increase of the actual displacement Δv and the displacement Δv_b which corresponds to pure bending, Fig. 2.

The *discrete* shear gap is defined at node i by integration of the discretized shear strains:

$$\Delta v_\gamma^i(x_1) = v_h|_{x_1}^{x_i} + \int_{x_1}^{x^i} \beta_h \, \mathrm{d}x = \int_{x_1}^{x^i} \gamma_h \, \mathrm{d}x \tag{4}$$

where x_i is the coordinate of node i. For the case of pure bending, the discretized Bernoulli (or Kirchhoff) condition means zero discrete shear gaps. This condition can be fulfilled, leading to the correct zero shear deformation. Although formulated for shear deformable beams the concept meets the discrete Kirchhoff idea for the case of pure bending.

After discretization of displacement and rotation field, in general, (1) does not apply anymore to determine the discretized shear deformation γ_h:

$$\gamma_h \neq v_h' + \beta_h \tag{5}$$

This is obvious in the case of pure bending. In particular, if displacement v_h and rotation β_h are interpolated

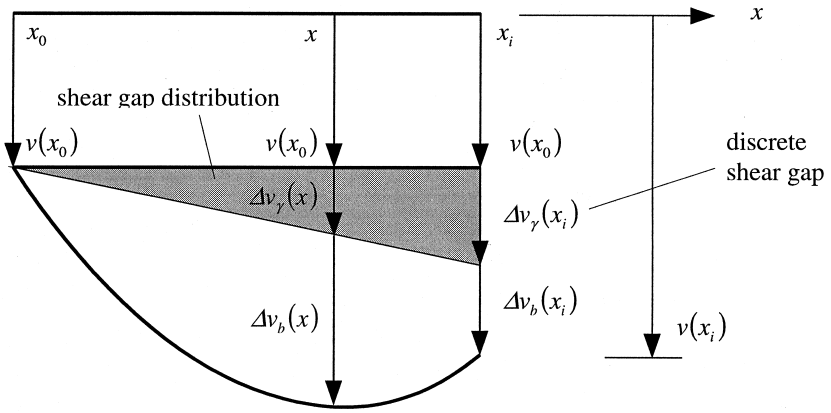

Fig. 2. Shear gap.

by the same functions — as it is usually the case — the difference of displacement gradient and rotation cannot anymore vanish identically, i.e. the Bernoulli (Kirchhoff) condition cannot be satisfied for pure bending:

$$0 \neq v_h' + \beta_h \tag{6}$$

If, however, (5) is used — although it is not valid but is usually done with standard displacement elements — any deformation, even pure bending, exhibits some parasitic shear. The element behaves too stiff; the effect is known as 'shear locking'.

As a consequence, the discretized shear deformation has to be formulated alternatively, e.g. in an integral sense by discretization of the shear gap (3). The idea is to represent the shear deformation by their equivalent part of the nodal displacements, the discrete shear gaps Δv_γ^i at the finite element nodes.

The discretized shear gap field is determined by interpolation of the nodal shear gaps:

$$\Delta v_\gamma = \sum_{i=1}^{N} N^i \Delta v_\gamma^i \tag{7}$$

N is the number of element nodes and N^i are the shape functions. The shear deformation is evaluated straightforward by differentiation:

$$\gamma_h = \sum_{i=1}^{N} \frac{\mathrm{d}N^i}{\mathrm{d}x} \Delta v_\gamma^i \tag{8}$$

By that means the shear deformation is consistently separated from the bending deformation and, therefore, the procedure could also be understood as a decomposition of shear and bending modes. However, this is the result of the formulation and was not a presumption as in other comparable approaches. In principle, the idea has been brought up in earlier contributions for beams as well as it is part of special formulations for plate and shell elements, as indicated in the introduction. The difference to the present concept is that now the procedure can be unified and equivalently applied to plates and shells. This will be demonstrated in the following sections.

The idea is put in concrete form by the example of a simple linear Timoshenko beam element, Fig. 3.

According to Eq. (4), the shear gap is evaluated at node i with coordinate x_i ($x_1 = 0$; $x_2 = l$):

$$\int_0^{x_i} \gamma_h(x)\,\mathrm{d}x = v_h|_0^{x_i} + \int_0^{x_i} \beta_h(x)\,\mathrm{d}x = \Delta v_\gamma^i \tag{9}$$

Since the shear strains alone are regarded, only the shear gap difference is of interest, the gap at node 1 which can be identified as the integration constant is set to zero. Hence

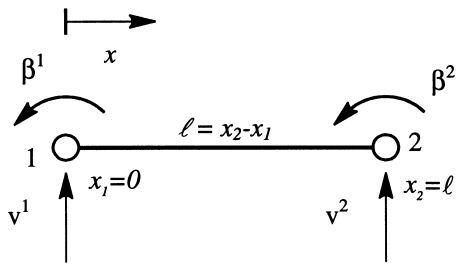

Fig. 3. Linear Timoshenko beam.

$$\Delta v_\gamma^1 = 0; \qquad \Delta v_\gamma^2 = v^2 - v^1 + \int_0^l \beta_h\,\mathrm{d}x \tag{10}$$

The discretized rotations are given by

$$\beta_h(x) = \sum_{i=1}^{2} N^i \cdot \beta^i = \frac{1}{l}(l-x)\beta^1 + \frac{1}{l}x\beta^2 \tag{11}$$

and with (10) we obtain

$$\begin{aligned}\Delta v_\gamma^2 &= v^2 - v^1 + \int_0^l N^1\,\mathrm{d}x \cdot \beta^1 + \int_0^l N^2\,\mathrm{d}x \cdot \beta^2 \\ &= v^2 - v^1 + \frac{l}{2}(\beta^1 + \beta^2)\end{aligned} \tag{12}$$

The distribution of the shear gap across the element is now calculated by interpolation from its nodal value with the standard shape functions N^i,

$$\begin{aligned}\Delta v_\gamma(x) &= \sum_{i=1}^{2} N^i \cdot \Delta v_\gamma^i \\ &= \frac{1}{l}x\left[v^2 - v^1 + \frac{l}{2}(\beta^1 + \beta^2)\right]\end{aligned} \tag{13}$$

Finally, the 'correct shear' is obtained by differentiating Δv_γ with respect to x.

$$\gamma(x) = \frac{\mathrm{d}\Delta v_\gamma(x)}{\mathrm{d}x} = \frac{1}{l}(v^2 - v^1) + \frac{1}{2}(\beta^1 + \beta^2) \tag{14}$$

Modification of the differential operator for the strains according to (14) leads to a shear-locking-free beam element. In fact, the resulting stiffness matrix is identical to that of a reduced integrated beam element. For comparison, the shear strains in the pure displacement element are

$$\gamma^d(x) = \frac{1}{l}(v^2 - v^1) + \frac{1}{l}(l-x)\beta^1 + \frac{x}{l} \cdot \beta^2 \tag{15}$$

Note, that only the part containing the rotations is affected by the procedure and that the undesired linear components in Eq. (15) do not show up in Eq. (14). In the case of curved beams (or shells, see Section 3) an

additional term evolves, that also affects the part containing the displacements v_i.

3. DSG-elements in curvilinear coordinates

3.1. Shell formulation including thickness stretch

The basic idea described above is now used to derive a class of shear deformable plate and shell elements, either triangular or rectangular, of arbitrary polynomial order. The underlying shell formulation is a seven-parameter model, including a thickness stretch of the shell. This model is feasible for implementation of arbitrary three-dimensional constitutive laws, and has been described extensively in Refs. [7,9]. The procedure to obtain the modified differential operator is exactly the same as in Section 2.

As the shell formulation at hand covers the fully three-dimensional stress and strain state, the strains can be expressed by the three-dimensional Green–Lagrange strain tensor $\mathbf{E}$

$$\mathbf{E} = E_{ij} \cdot \mathbf{g}^i \otimes \mathbf{g}^j; \quad E_{ij} = \frac{1}{2}\left(\bar{\mathbf{g}}_i \bar{\mathbf{g}}_j - \mathbf{g}_i \mathbf{g}_j\right) \tag{16}$$

Here, $\mathbf{g}_i$ and $\mathbf{g}^i$ are the co- and contravariant base vectors of the shell body, respectively. The covariant base vectors in the undeformed and deformed configuration, respectively, are given by

$$\mathbf{g}_\alpha = \frac{\partial \mathbf{x}}{\partial \theta^\alpha} = \mathbf{x}_{,\alpha}; \qquad \bar{\mathbf{g}}_\alpha = \bar{\mathbf{x}}_{,\alpha} \tag{17}$$

Note that Greek indices run from 1 to 2, Latin indices run from 1 to 3. Unless otherwise stated, we will make use of Einstein's summation convention. A bar denotes variables in the deformed configuration.

The geometry of the shell in the undeformed and the deformed state is represented by

$$\mathbf{x} = \mathbf{r} + \theta^3 \cdot \mathbf{a}_3; \quad \mathbf{a}_3 = \frac{h}{2} \cdot \frac{\mathbf{a}_1 \times \mathbf{a}_2}{|\mathbf{a}_1 \times \mathbf{a}_2|}; \quad \mathbf{a}_\alpha = \mathbf{r}_{,\alpha} \tag{18}$$

$$\bar{\mathbf{a}}_\alpha = \bar{\mathbf{r}}_{,\alpha} = \mathbf{a}_\alpha + \mathbf{v}_{,\alpha} \tag{19}$$

$$\bar{\mathbf{a}}_3 = \mathbf{a}_3 + \mathbf{w} \tag{20}$$

i.e. the position vector $\boldsymbol{x}$ to any arbitrary point of the shell can be expressed by the position vector $\boldsymbol{r}$ to a reference point on the midsurface of the shell and the so-called 'director' $\mathbf{a}_3$, Fig. 4. The position vector of a point in the deformed configuration is given by

$$\bar{\mathbf{x}} = \bar{\mathbf{r}} + \theta^3 \cdot \bar{\mathbf{a}}_3 \tag{21}$$

and thus, the deformation can be described as

$$\begin{aligned} &\mathbf{u} = \mathbf{v} + \theta^3 \cdot \mathbf{w} \rightarrow \bar{\mathbf{x}} = \mathbf{x} + \mathbf{u}; \quad \bar{\mathbf{r}} = \mathbf{r} + \mathbf{v}; \\ &\bar{\mathbf{a}}_3 = \mathbf{a}_3 + \mathbf{w} \end{aligned} \tag{22}$$

In contrast to a classical Reissner–Mindlin type five-parameter plate or shell formulation, the update of the director is formulated through the difference vector $\mathbf{w}$ instead of a rotation tensor. The three independent components of the difference vector allow for a change of direction of the director $\mathbf{a}_3$ as well as a change of its length.

To avoid a certain 'thickness locking' phenomenon, the formulation with six parameters has to be further

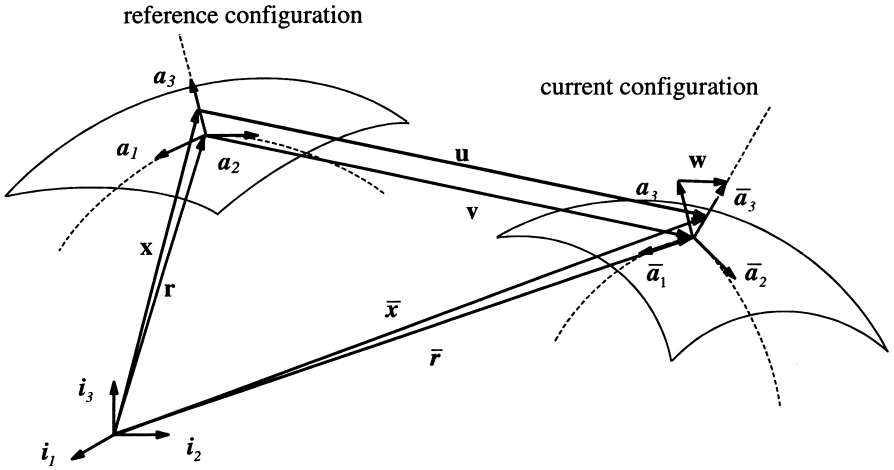

Fig. 4. Geometry and kinematics of the shell.

enhanced by a seventh parameter, introducing a linear varying normal strain in thickness direction. This can be achieved either indirectly, by rising the polynomial order of the displacements [18,22] or directly via a hybrid mixed method. A possibility to introduce this parameter with the help of the Enhanced Assumed Strain (EAS) method has been described by Büchter and Ramm [9]. For details see also Büchter et al. [10] and Bischoff and Ramm [7].

Another thickness locking phenomenon, termed 'curvature thickness locking', can be overcome with the help of an ANS approach [6,7,21]. It should be noted, that both thickness locking effects are consequences of the special shell formulation and do not appear in a 'classical' five-parameter shell formulation.

For the calculation of the strain, the covariant base vectors of the shell body are needed in terms of the mid-surface.

$$\bar{\mathbf{g}}_i = \bar{\mathbf{x}}_{,i} = \mathbf{x}_{,i} + \mathbf{u}_{,i} = \mathbf{g}_i + \mathbf{u}_{,i} \tag{23}$$

$$\bar{\mathbf{g}}_\alpha = \mathbf{g}_\alpha + \mathbf{v}_{,\alpha} + \theta^3 \mathbf{w}_{,\alpha}; \qquad \bar{\mathbf{g}}_3 = \mathbf{g}_3 + \mathbf{w} \tag{24}$$

With

$$\mathbf{g}_\alpha = \mathbf{x}_{,\alpha} = \mathbf{a}_\alpha + \theta^3 \mathbf{a}_{3,\,\alpha}; \quad \mathbf{g}_3 = \mathbf{a}_3 \tag{25}$$

we finally obtain expressions for the strain tensor components as $E_{ij} \approx \alpha_{ij} + \theta^3 \beta_{ij}$, with

$$\alpha_{ij} = \frac{1}{2}\left(\bar{\mathbf{a}}_i \bar{\mathbf{a}}_j - \mathbf{a}_i \mathbf{a}_j\right) \tag{26}$$

$$\beta_{\alpha\beta} = \frac{1}{2}\left(\bar{\mathbf{a}}_\alpha \bar{\mathbf{a}}_{3,\,\beta} + \bar{\mathbf{a}}_\beta \bar{\mathbf{a}}_{3,\,\alpha} - \mathbf{a}_\alpha \mathbf{a}_{3,\,\beta} - \mathbf{a}_\beta \mathbf{a}_{3,\,\alpha}\right) \tag{27}$$

$$\beta_{\alpha 3} = \frac{1}{2}\left(\bar{\mathbf{a}}_{3,\,\alpha} \bar{\mathbf{a}}_3 - \mathbf{a}_{3,\,\alpha} \mathbf{a}_3\right); \beta_{33} = 0 \tag{28}$$

Discretization of geometry and displacements

$$\mathbf{r} = \sum_{n=1}^{N} N^n \mathbf{x}^n; \quad \mathbf{v} = \sum_{n=1}^{N} N^n \mathbf{v}^n; \quad \mathbf{w} = \sum_{n=1}^{N} N^n \mathbf{w}^n \tag{29}$$

leads to the covariant base vectors of the midsurface in discrete form

$$\mathbf{a}_1 = \sum_{n=1}^{N} \frac{\partial N^n}{\partial \xi} \mathbf{x}^n; \qquad \mathbf{a}_2 = \sum_{n=1}^{N} \frac{\partial N^n}{\partial \eta} \mathbf{x}^n \tag{30}$$

$$\bar{\mathbf{a}}_1 = \mathbf{a}_1 + \sum_{n=1}^{N} \frac{\partial N^n}{\partial \xi} \mathbf{v}^n; \qquad \bar{\mathbf{a}}_2 = \mathbf{a}_2 + \sum_{n=1}^{N} \frac{\partial N^n}{\partial \eta} \mathbf{v}^n \tag{31}$$

The shell 'director' is calculated as follows. First, at each element node the normal vector to the discretized shell surface is calculated:

$$\tilde{\mathbf{a}}_3^n = \frac{h}{2} \frac{\mathbf{a}_1^n \times \mathbf{a}_2^n}{|\mathbf{a}_1^n \times \mathbf{a}_2^n|} \tag{32}$$

Then, the different directors $\tilde{\mathbf{a}}_3^n$ of common nodes of adjacent elements are averaged to yield one director per node:

$$\mathbf{a}_3^n = \frac{1}{nel} \cdot \sum_{n=1}^{nel} \tilde{\mathbf{a}}_3^n; \quad nel = \text{no. of adjacent elements} \tag{33}$$

The director field within one element can now be expressed as:

$$\mathbf{a}_3 = \sum_{n=1}^{N} N^n \cdot \mathbf{a}_3^n; \qquad \bar{\mathbf{a}}_3 = \mathbf{a}_3 + \sum_{n=1}^{N} N^n \cdot \mathbf{w}^n \tag{34}$$

The constant part of the transverse shear strains is due to (26)

$$\begin{aligned} \alpha_{\alpha 3} &= \frac{1}{2}(\bar{\mathbf{a}}_\alpha \bar{\mathbf{a}}_3 - \mathbf{a}_\alpha \mathbf{a}_3) \\ &= \frac{1}{2}\left[(\mathbf{a}_\alpha + \mathbf{v}_{,\alpha})(\mathbf{a}_3 + \mathbf{w}) - \mathbf{a}_\alpha \mathbf{a}_3\right] \end{aligned} \tag{35}$$

For geometrically linear problems the terms, which are quadratic in the displacements, are neglected, thus

$$\alpha_{\alpha 3} = \frac{1}{2}(\mathbf{a}_\alpha \mathbf{w} + \mathbf{a}_3 \mathbf{v}_\alpha) \tag{36}$$

The linear part of the transverse shear strain $\beta_{\alpha 3}$ does not contribute to the shear locking phenomenon and remains, therefore, unchanged.

3.2. Modification of shear strains for DSG elements

Now, the same steps as for the derivation of the beam element in Section 2 are performed. First, the discrete shear gaps are evaluated by integrating the transverse shear strains (36) over the element domain.

$$\Delta v_{\gamma 1}^i = \int_{\xi_1}^{\xi_i} \alpha_{13}\, \mathrm{d}\xi; \qquad \Delta v_{\gamma 2}^i = \int_{\eta_1}^{\eta_i} \alpha_{23}\, \mathrm{d}\eta \tag{37}$$

Here, ξ_i; η_i are the natural coordinates of node i, $\Delta v_{\gamma\alpha}^i$ is the discrete shear gap associated with the α-direction. Introducing (36) into (37) yields

$$\begin{aligned} \Delta v_{\gamma 1}^i &= \frac{1}{2} \int_{\xi_1}^{\xi_i} [\mathbf{a}_3 \mathbf{v}_{,1} + \mathbf{a}_1 \mathbf{w}]\, \mathrm{d}\xi \\ &= \frac{1}{2} \int_{\xi_1}^{\xi_i} [\mathbf{a}_3 \mathbf{v}_{,1} + \mathbf{r}_{,1} \mathbf{w}] \mathrm{d}\xi = \Delta v_{v1}^i + \Delta v_{w1}^i \end{aligned} \tag{38}$$

$$\Delta v^i_{\gamma 2} = \frac{1}{2}\int_{\eta_1}^{\eta_i} [\mathbf{a}_3 \mathbf{v}_{,2} + \mathbf{a}_2 \mathbf{w}]\, \mathrm{d}\eta$$

$$= \frac{1}{2}\int_{\eta_1}^{\eta_i} [\mathbf{a}_3 \mathbf{v}_{,2} + \mathbf{r}_{,2} \mathbf{w}] \mathrm{d}\eta = \Delta v^i_{v2} + \Delta v^i_{w2} \tag{39}$$

The decisive advantage of the procedure is that the integrals in Eqs. (38) and (39) can be determined analytically a priori, e.g. by the proper use of computer algebra packages (see Section 4.1 for a three-node element). This leads to a very compact and efficient program code.

Discretization of the displacement vectors $\mathbf{v}$ and $\mathbf{w}$

$$\mathbf{v} = \sum_{n=1}^{N} N^n(\xi,\eta)\mathbf{v}^n; \qquad \mathbf{w} = \sum_{n=1}^{N} N^n(\xi,\eta)\mathbf{w}^n \tag{40}$$

leads to the following expressions for the *discrete shear gap* at node i (coordinates ξ_i; η_i).

$$\Delta v^i_{v1} = \frac{1}{2}\int_{\xi_1}^{\xi_i} \left[\sum_{n=1}^{N} \frac{\partial N^n}{\partial \xi}(\xi,\eta_i)\mathbf{v}^n \cdot \sum_{n=1}^{N} N^n(\xi,\eta_i)\mathbf{a}^n_3 \right] \mathrm{d}\xi \tag{41}$$

$$\Delta v^i_{v2} = \frac{1}{2}\int_{\eta_1}^{\eta_i} \left[\sum_{n=1}^{N} \frac{n}{\partial \eta}(\xi_i,\eta)\mathbf{v}^n \cdot \sum_{n=1}^{N} N^n(\xi_i,\eta)\mathbf{a}^n_3 \right] \mathrm{d}\eta \tag{42}$$

$$\Delta v^i_{w1} = \frac{1}{2}\int_{\xi_1}^{\xi_i} \left[\sum_{n=1}^{N} \frac{\partial N^n}{\partial \xi}(\xi,\eta_i)\mathbf{r}^n \cdot \sum_{n=1}^{N} N^n(\xi,\eta_i)\mathbf{w}^n \right] \mathrm{d}\xi \tag{43}$$

$$\Delta v^i_{w2} = \frac{1}{2}\int_{\eta_1}^{\eta_i} \left[\sum_{n=1}^{N} \frac{\partial N^n}{\partial \eta}(\xi_i,\eta)\mathbf{r}^n \cdot \sum_{n=1}^{N} N^n(\xi_i,\eta)\mathbf{w}^n \right] \mathrm{d}\eta \tag{44}$$

According to Eq. (13) the next step is the interpolation of the discrete shear gaps across the element.

$$\Delta v_{\gamma 1}(\xi,\eta) = \sum_{n=1}^{N} \left(N^n(\xi,\eta) \cdot \Delta v^n_{\gamma 1} \right) \tag{45}$$

$$\Delta v_{\gamma 2}(\xi,\eta) = \sum_{n=1}^{N} \left(N^n(\xi,\eta) \cdot \Delta v^n_{\gamma 2} \right) \tag{46}$$

The modified shear strains are finally obtained via partial differentiation of the shear gap distribution.

$$\gamma_\xi = \frac{\partial \Delta v_{\gamma 1}(\xi,\eta)}{\partial \xi} = \sum_{n=1}^{N} \left(\frac{\partial N^n}{\partial \xi} \cdot \Delta v^n_{\gamma 1} \right) \tag{47}$$

$$\gamma_\eta = \frac{\partial \Delta v_{\gamma 2}(\xi,\eta)}{\partial \eta} = \sum_{n=1}^{N} \left(\frac{\partial N^n}{\partial \eta} \cdot \Delta v^n_{\gamma 2} \right) \tag{48}$$

These formulae apply to any kind of element, either triangles or rectangles of arbitrary polynomial order. The only modification that has to be carried out to obtain a DSG-element in an existing code for pure displacement elements, is to replace the corresponding part in the differential operator matrix $\mathbf{B}$ by Eqs. (47) and (48).

It should be mentioned that the formulae have been derived without considering conforming displacements at the element interfaces, thus violating the principle of virtual work. However, in the case of quadrilateral elements the formulation leads to well known and accepted results, as there is a variational justification for ANS elements (see Ref. [26]). For triangular elements the formulation still misses a rigid mathematical justification, however, the elements pass the patch test and are free of spurious kinematic modes.

Further, the idea of discrete shear gaps introduces nodal indicators of shear deformation or, for thin elements, discrete Kirchhoff constraints at the element nodes. This means that for any specific element the constraint count [14] has always the ideal number.

4. Element matrices

4.1. Three-node triangular element

4.1.1. Curvilinear coordinates

As an example, a three-node DSG-element is derived.

Geometry and shape functions, as well as their derivatives are given for a three-node element in Fig. 5. The discrete shear gaps at the nodes are calculated according to Eqs. (41)–(44)

$$\Delta v^1_{v1} = 0; \quad \Delta v^2_{v1} = \frac{1}{4}(\mathbf{v}^2 - \mathbf{v}^1) \cdot (\mathbf{a}^1_3 + \mathbf{a}^2_3); \quad \Delta v^3_{v1} = 0$$

$$\Delta v^1_{v2} = 0; \quad \Delta v^3_{v2} = \frac{1}{4}(\mathbf{v}^3 - \mathbf{v}^1) \cdot (\mathbf{a}^1_3 + \mathbf{a}^3_3); \quad \Delta v^2_{v2} = 0$$

$$\Delta v^1_{w1} = 0; \quad \Delta v^2_{w1} = \frac{1}{4}(\mathbf{r}^2 - \mathbf{r}^1) \cdot (\mathbf{w}^1 + \mathbf{w}^2); \quad \Delta v^3_{w1} = 0$$

$$\Delta v^1_{w2} = 0; \quad \Delta v^3_{w2} = \frac{1}{4}(\mathbf{r}^3 - \mathbf{r}^1) \cdot (\mathbf{w}^1 + \mathbf{w}^3); \quad \Delta v^2_{w2} = 0$$

The modified shear strains for the three node elements are consequently

$$\gamma_\xi = \frac{1}{4}\left[(\mathbf{v}^2 - \mathbf{v}^1) \cdot (\mathbf{a}^1_3 + \mathbf{a}^2_3) + (\mathbf{r}^2 - \mathbf{r}^1) \cdot (\mathbf{w}^1 + \mathbf{w}^2) \right] \tag{49}$$

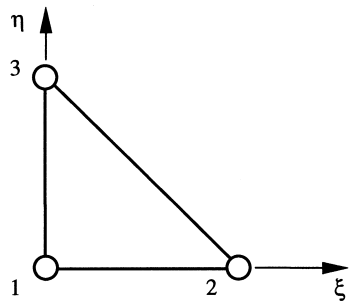

$$\xi_1 = 0 \quad \eta_1 = 0 \quad N_1 = 1-\xi-\eta$$
$$\xi_2 = 1 \quad \eta_2 = 0 \quad N_2 = \xi$$
$$\xi_3 = 0 \quad \eta_3 = 1 \quad N_3 = \eta$$
$$()_{,\xi} = \frac{\partial()}{\partial\xi} \quad N_{1,\xi} = -1 \quad N_{1,\eta} = -1$$
$$N_{2,\xi} = 1 \quad N_{2,\eta} = 0$$
$$()_{,\eta} = \frac{\partial()}{\partial\eta} \quad N_{3,\xi} = 0 \quad N_{3,\eta} = 1$$

Fig. 5. Three-node element.

$$\gamma_\eta = \frac{1}{4}\left[(\mathbf{v}^3 - \mathbf{v}^1)\cdot(\mathbf{a}_3^1 + \mathbf{a}_3^3) + (\mathbf{r}^3 - \mathbf{r}^1)\cdot(\mathbf{w}^1 + \mathbf{w}^3)\right] \tag{50}$$

In contrast to the pure displacement element, where the shear strains are linearly varying across the element, they are constant in this formulation. The spurious linear components which are responsible for shear locking are effectively eliminated, independent of the element shape.

As for the linear beam element and the bi-linear plate element, the procedure could be interpreted as an averaging of the transverse shear strains along the edges [16], this is obviously not true in the case of the linear triangle, where, only two edges are taken into account. This is the decisive difference to the KM-element, introduced by Hughes and Taylor [15], where explicit satisfaction of the Kirchhoff condition is introduced along all three edges leading to an artificial constraint. The resulting element is consequently not free of shear locking.

As a result, the element stiffness matrices of triangular DSG-elements depend on the sequence of node numbers (see Eq. (57)). The influence on the solution, however, diminishes with mesh refinement as satisfaction of the patch test is ensured anyhow. It should be noted that this unusual loss of objectivity of the element formulation is in no way a result of any specific construction for three node elements, but comes along quite naturally with a consequent application of the DSG-concept. In fact, it can be observed that the attempt to treat all three edges of a triangle equally turns out to be a major obstacle in the construction of locking-free elements. Therefore, the DSG-concept merely takes care of coordinate directions instead of element edges.

Additionally, an alternative formulation of a three node element insensitive to node numbering should be mentioned, which is given in the ABAQUS theory manual [13] and was presented by Fox and Nagtegaal [11]. The element is defined as the result of a collapsed bilinear, reduced integrated quadrilateral with hourglas stabilization. The shear strain is derived from a modification of the Bathe–Dvorkin ANS-scheme with respect to the hourglass modes of shear deformation.

4.1.2. Plate element in Cartesian coordinates

To demonstrate the simplicity and efficiency of the presented method, a closed form **B**-operator matrix for the DSG3 plate element is given in this section. It relies on a classical five-parameter formulation with rotations β_x and β_y instead of the difference vector used in Section 3.

The element is defined as shown in Fig. 6. Geometry, deflections and rotations are interpolated by the same shape functions:

$$\begin{Bmatrix} x \\ y \\ v \\ \beta_x \\ \beta_y \end{Bmatrix} = \sum_{i=1}^{3} N_i \begin{Bmatrix} x^i \\ y^i \\ v^i \\ \beta_x^i \\ \beta_y^i \end{Bmatrix}; \qquad \begin{matrix} N_1 = 1-\xi-\eta \\ N_2 = \xi \\ N_3 = \eta \end{matrix} \tag{51}$$

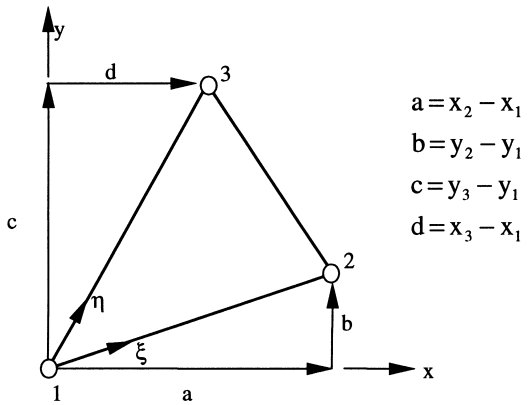

$$a = x_2 - x_1$$
$$b = y_2 - y_1$$
$$c = y_3 - y_1$$
$$d = x_3 - x_1$$

Fig. 6. Three-node element.

The Jacobian matrix and its inverse are determined to be:

$$\mathbf{J} = \begin{bmatrix} x_{,\xi} & y_{,\xi} \\ x_{,\eta} & y_{,\eta} \end{bmatrix} = \begin{bmatrix} a & b \\ d & c \end{bmatrix}$$
$$\mathbf{J}^{-1} = \begin{bmatrix} \xi_{,x} & \eta_{,x} \\ \xi_{,y} & \eta_{,y} \end{bmatrix} = \frac{1}{\det J}\begin{bmatrix} c & -b \\ -d & a \end{bmatrix}; \quad \det J = ac - bd = 2A \tag{52}$$

Next, the 'shear gap' distributions are calculated:

$$\Delta v_{\gamma 1} = v(\xi,\eta)|_{\xi_1}^{\xi_i} + \int_{\xi_1}^{\xi_i} (\beta_x a + \beta_y b)\, \mathrm{d}\xi$$

$$= \left[v(\xi,\eta) + a\left\{ \left(\xi - \frac{1}{2}\xi^2 - \xi\eta \right)\beta_x^1 + \frac{1}{2}\xi^2\beta_x^2 + \xi\eta\beta_x^3 \right\} \right]_{\xi_1}^{\xi_i}$$

$$+ \left[b\left\{ \left(\xi - \frac{1}{2}\xi^2 - \xi\eta \right)\beta_y^1 + \frac{1}{2}\xi^2\beta_y^2 + \xi\eta\beta_y^3 \right\} \right]_{\xi_1}^{\xi_i} \tag{53}$$

and

$$\Delta v_{\gamma 2} = v(\xi,\eta)|_{\eta_1}^{\eta_i} + \int_{\eta_1}^{\eta_i} (\beta_x d + \beta_y c)\, \mathrm{d}\xi$$

$$= \left[v(\xi,\eta) + d\left\{ \left(\eta - \xi\eta - \frac{1}{2}\eta^2 \right)\beta_x^1 + \xi\eta\beta_x^2 + \frac{1}{2}\eta^2\beta_x^3 \right\} \right]_{\eta_1}^{\eta_i}$$

$$+ \left[b\left\{ \left(\eta - \xi\eta - \frac{1}{2}\eta^2 \right)\beta_y^1 + \xi\eta\beta_y^2 + \frac{1}{2}\eta^2\beta_y^3 \right\} \right]_{\eta_1}^{\eta_i} \tag{54}$$

It has been assumed that the axes of rotation for β_x and β_y do not change within the element. Thus, the formulation is, strictly speaking, not valid for shells, although the described element accounts for membrane action. However, the present element could be applied as a piecewise plane 'facet element' also for the analysis of shells, provided no average director (see Section 3) is used.

At the nodes the discrete shear gaps are evaluated to be

$$\Delta v_{\gamma 1}^1 = \Delta v_{\gamma 1}^3 = \Delta v_{\gamma 2}^1 = \Delta v_{\gamma 2}^2 = 0$$

$$\Delta v_{\gamma 1}^2 = (v^2 - v^1) + \frac{1}{2}a\left(\beta_x^1 + \beta_x^2\right) + \frac{1}{2}b\left(\beta_y^1 + \beta_y^2\right)$$

$$\Delta v_{\gamma 2}^3 = (v^3 - v^1) + \frac{1}{2}d\left(\beta_x^1 + \beta_x^3\right) + \frac{1}{2}c\left(\beta_y^1 + \beta_y^3\right) \tag{55}$$

from which the modified interpolation scheme for the shear strain results:

$$\gamma_x = \frac{\partial N_2}{\partial \xi}\frac{\partial \xi}{\partial x}\Delta v_{\gamma 1}^2 + \frac{\partial N_3}{\partial \eta}\frac{\partial \eta}{\partial x}\Delta v_{\gamma 1}^3 \Delta v_{\gamma 2}^3$$

$$\gamma_y = \frac{\partial N_2}{\partial \xi}\frac{\partial \xi}{\partial y}\Delta v_{\gamma 2}^2 \Delta v_{\gamma 1}^2 + \frac{\partial N_3}{\partial \eta}\frac{\partial \eta}{\partial y}\Delta v_{\gamma 2}^3 \tag{56}$$

Finally, the differential operator **B** can be derived to determine curvature and shear deformations from nodal displacements and rotations:

$$(\kappa_x, \kappa_y, \kappa_{xy}, \gamma_x, \gamma_y)^{\mathrm{T}} = \mathbf{B}\mathbf{u}$$
$$= \mathbf{B}\left(w^1, \beta_x^1, \beta_y^1, w^2, \beta_x^2, \beta_y^2, w^3, \beta_x^3, \beta_y^3\right)^{\mathrm{T}}$$

$$\mathbf{B} = \frac{1}{\det J}\left[\begin{array}{ccc|ccc|ccc} 0 & b-c & 0 & 0 & c & 0 & 0 & -b & 0 \\ 0 & 0 & d-a & 0 & 0 & -d & 0 & 0 & a \\ 0 & d-a & b-c & 0 & -d & c & 0 & a & -b \\ b-c & \frac{1}{2}\det J & 0 & c & \frac{ac}{2} & \frac{bc}{2} & -b & -\frac{bd}{2} & -\frac{bc}{2} \\ d-a & 0 & \frac{1}{2}\det J & -d & -\frac{ad}{2} & -\frac{bd}{2} & a & \frac{ad}{2} & \frac{ac}{2} \end{array}\right] \tag{57}$$

The stiffness matrix **K** and the stresses σ are determined by the standard finite element relations:

$$\mathbf{K} = \int_V \mathbf{B}^{\mathrm{T}}\mathbf{D}\mathbf{B}\, \mathrm{d}V; \qquad \sigma = \mathbf{D}\mathbf{B}\mathbf{u} \tag{58}$$

where **D** is the constitutive matrix of plate bending and **u** is the vector of generalized nodal displacements. Note, that the proposed formulation results in a simple modification of the **B**-operator compared to the original displacement element. In the special case of the three node element, the **B**-operator is even a constant matrix, i.e. the volume integration in (58) can be performed analyti-

cally or numerically by a one point Gauss quadrature. Again, compared to the original displacement formulation, the order of integration can be reduced without activating zero energy modes. This result can be generalized, i.e. the order of integration can be reduced by one for any triangle or selectively for the integration of the shear deformation parts of quadrilateral elements which leads to considerable enhancements of efficiency.

4.2. Four-node quadrilateral

Analogous to the development of a three-node element, a bilinear four-node element can be derived, Fig. 7. Rectangular elements are usually superior to triangles with respect to the rate of convergence.

Application of Eqs. (47) and (48) leads to the following shear strain distributions for the DSG4 element.

$$\gamma_\xi = \frac{1}{4}(1-\eta)\left[\left(\mathbf{v}^2\mathbf{a}_3^2 - \mathbf{v}^1\mathbf{a}_3^1\right) + \left(\mathbf{w}^1 + \mathbf{w}^2\right)\left(r^2 - r^1\right)\right] + \frac{1}{4}(1+\eta)\left[\left(\mathbf{v}^3\mathbf{a}_3^3 - \mathbf{v}^4\mathbf{a}_3^4\right) + \left(\mathbf{w}^3 + \mathbf{w}^4\right)\left(\mathbf{r}^3 - \mathbf{r}^4\right)\right] \tag{59}$$

$$\gamma_\eta = \frac{1}{4}(1-\xi)\left[\left(\mathbf{v}^4\mathbf{a}_3^4 - \mathbf{v}^1\mathbf{a}_3^1\right) + \left(\mathbf{w}^1 + \mathbf{w}^4\right)\left(\mathbf{r}^4 - \mathbf{r}^1\right)\right] + \frac{1}{4}(1+\xi)\left[\left(\mathbf{v}^3\mathbf{a}_3^3 - \mathbf{v}^2\mathbf{a}_3^2\right) + \left(\mathbf{w}^3 + \mathbf{w}^2\right)\left(\mathbf{r}^3 - \mathbf{r}^2\right)\right] \tag{60}$$

Note, that these linear-constant distributions of shear strains are exactly the ones obtained by application of the classical ANS method [4,16]. In fact, the resulting stiffness matrix is identical to the one of the 'Bathe–Dvorkin' element, even for arbitrarily distorted elements.

4.3. Six-node triangle

In practical engineering applications low-order elements are usually preferred. Nevertheless, there are several reasons speaking for the use of higher order elements. Given a certain number of dof, the accuracy of the results is usually significantly better when using higher order elements. In addition, higher order elements are not as sensitive with respect to *linear* mesh distortions. *Quadratically* distorted meshes can be avoided by a sub-parametric interpolation of the geometry in the geometrical linear case.

It can be seen from the numerical investigations in Section 5.1, that the DSG6-element exhibits a tremendous rate of convergence, although the elements are quadratically distorted due to the circular shape of the structure.

4.4. Nine-node quadrilateral

The nine node DSG9-element has again some similarities to the corresponding ANS-element (e.g. ref [20]). For rectangular and linearly distorted elements, the stiffness matrices are again identical (cf. Section 4.3), for quadratic distortions the stiffness matrices are slightly different. However, these differences are practically not significant.

The main merit of the nine-node element is robustness, rather than efficiency. Even in the case of quadratically distorted meshes, performance is excellent. For the application to shells, a modification of the membrane part is recommended to avoid in-plane shear locking and membrane locking. To achieve this, one possibility is the use of the Enhanced Assumed Strain (EAS) method, introduced by Simo and Rifai [23,24], and first applied to four-node, linear shell elements by Andelfinger and Ramm [1]. An application of the method, leading to extremely robust and reliable nine-node shell elements for geometrical non-linearity has been described by Bischoff and Ramm [7].

5. Numerical investigations

In order to examine the presented elements with

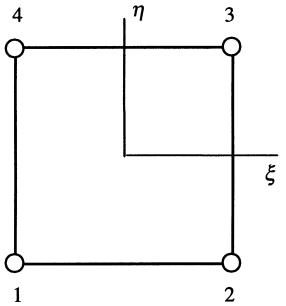

$$N^1 = \frac{1}{4}(1-\xi)(1-\eta)$$
$$N^2 = \frac{1}{4}(1+\xi)(1-\eta)$$
$$N^3 = \frac{1}{4}(1+\xi)(1+\eta)$$
$$N^4 = \frac{1}{4}(1-\xi)(1+\eta)$$

Fig. 7. Four-node element.

respect to efficiency, reference is made to some of the most successful triangular and rectangular elements known to the authors.

The triangular element of Xu [27] was the first locking-free triangular element with nine dof. The additional dof of the nodes at the midpoints and the two bubble modes for the rotations can be condensed on the element level. Thus, the total number of 9 dof per element is preserved.

The DST element (Discrete Shear Triangle) of Batoz and Katili [5], is an extension of the successful DKT element ('Discrete Kirchhoff Triangle'), introducing the effect of transverse shear deformations. The derivation of the element matrices is very elaborate; the basic feature is the calculation of the shear strains from the bending moments. Thus, shear locking effects are completely avoided, but convergence of the shear strains is poor.

As a member of the ANS- or MITC-family, the six-node MITC7 element of Bathe et al. [3] is also examined. The basic idea for the element formulation follows the concept of the four-node element of Bathe and Dvorkin [4]. In addition to the mixed interpolation of shear strains, a bubble mode is introduced. It should be mentioned that the computational cost for the calculation of the element stiffness matrix is very high, furthermore, a six-point quadrature is necessary for its numerical integration (eigenvalue analyses, however, show that even a four point quadrature does not produce any kinematic modes). In the present study, a six-point integration rule is applied.

The only rectangular element we refer to is the well known MITC4 element of Bathe and Dvorkin [4] which is based on the ANS method (see also Ref. [16]), already discussed in Section 1.

5.1. Circular plate

This simple example has two advantages. Firstly, an analytical solution for the Kirchhoff theory is available, and second, although the geometry is regular, the mesh is 'automatically' distorted, and there is no need for arbitrary, artificial mesh distortions to test the sensitivity of the elements (Fig. 8). The analytical solution is [25]:

$$w = \frac{pr^4}{64D}; \qquad D = \frac{Et^3}{12(1-\nu^2)} \Longrightarrow w \approx 0.010731 \frac{1}{t^3} = 10.731 \tag{61}$$

The elements are tested for an extremely thin plate (slenderness 1:500) and compared to some of the most popular and efficient elements known to the authors. Certainly, the given slenderness is outside the range of practical significance and applicability of a linear plate theory. This geometry is merely chosen to have a strong tendency to shear locking, thus demonstrating the benefit of the proposed method. Using symmetry, only one quarter of the system has been analyzed. The results are compiled in Table 1.

It can be seen that the present elements are among the best available triangular plate bending elements available to date. Especially the six-node element shows a rapid convergence to the final solution. Note that the Kirchhoff solution neglects the influence of transverse shear deformations, thus the analytical solution for a Reissner/Mindlin kinematics leads to slightly larger deformations.

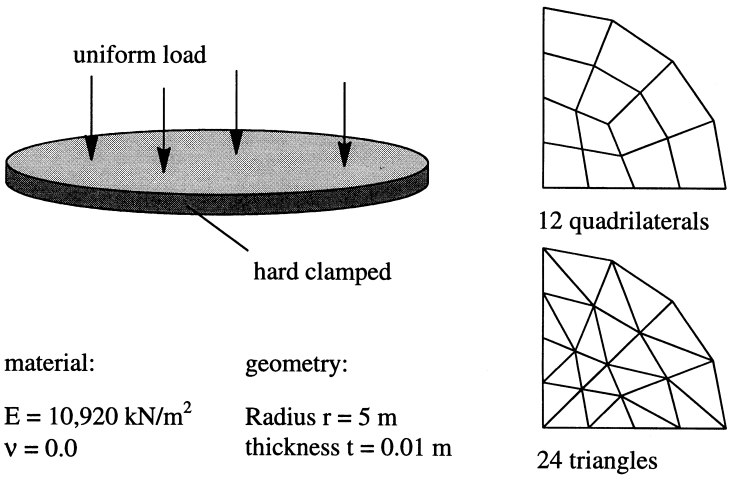

Fig. 8. Circular plate under uniform load-system and discretization.

Table 1
Circular plate — results

Number of nodes	DSG-3 (3-node)	Xu (3-node)	DST (3-node)	DSG-4 (4-node)	DSG-6 (6-node)	MITC7 (6-node)
19	10.324	9.844	10.949	10.653	10.828	8.479
61	10.632	10.514	10.793	10.715	10.739	10.162
127	10.687	10.636	10.759	10.724	10.733	10.481
217	10.707	10.678	10.747	10.728	10.732	10.591
331	10.716	10.698	10.742	10.729	10.732	10.642
469	10.721	10.708	10.739	10.730	10.732	10.670
631	10.724	10.714	10.737	10.730	10.732	10.686

In Fig. 9 the center displacement of the plate is plotted versus the number of nodes. On the left diagram it can be seen that all curves approach the Kirchhoff solution with increasing number of nodes. The different scale on the right diagram makes the excellent performance of the DSG-elements even more obvious. Here, also the results of the DSG4-element (identical to those of the ANS element of Bathe and Dvorkin [4]) are added, demonstrating the superiority of rectangular to triangular elements in the rate of convergence.

5.2. Cylindrical shell ('Scordelis-Lo Roof')

This cylindrical shell under dead load is an often used benchmark problem for linear and non-linear shell analysis. One advantage is, that — in contrast to many other benchmarks — there are no singularities involved.

The shell is analyzed using different discretizations with DSG3- and DSG4-elements in the setting of the three-dimensional shell formulation described in Section 3. For comparison, results obtained by the triangular DST and Xu elements are added. Due to the fact that these are based on a classical five-parameter formulation, there are slight deviations in the final results for the rather thick shell as can be seen on the right-hand side in Fig. 10. Nevertheless, it can be concluded that also in this example the DSG-elements are competitive with well established formulations.

While comparing the results, one should be aware that for a fixed number of nodes, the Xu and DST elements are significantly more expensive with respect to computation time. The reason for that is the fact that more quadrature points are needed for proper integration of the element matrices and additional dof are involved, which have to be condensed out on the element level.

The reader might recognize that the overall results of all elements tested in this example are relatively poor. This, however, is due to the fact that — for the sake of comparability — no additional efforts have been undertaken to improve the membrane behavior of the elements and to remove membrane locking. For quadrilateral elements this could be achieved by application of the EAS method. For triangles, a combi-

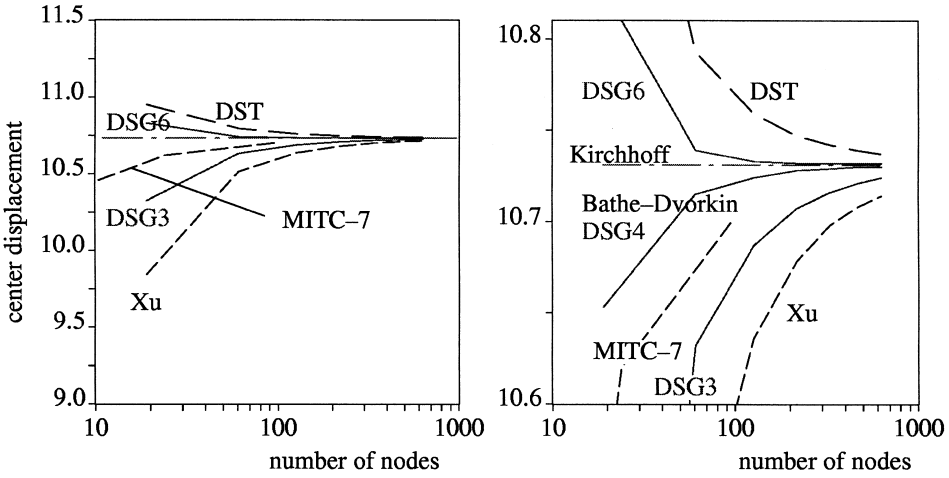

Fig. 9. Circular plate — results.

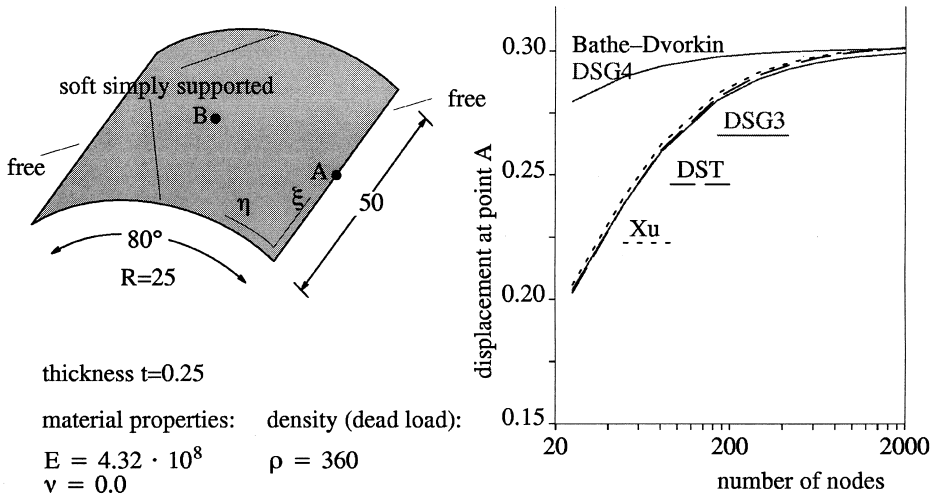

Fig. 10. Circular plate — results.

nation of EAS and the so-called 'free formulation' is successful (see Ref. [12] for an overview).

6. Conclusions

A unified formulation of shear-locking-free, Reissner/Mindlin plate and shell, rectangular and triangular finite elements has been presented. The method is based on the decomposition of bending and shear deformation. The presence of shear is identified by a nodal criterion. It compares the actual nodal displacements and displacements which are related to a pure bending mode. The difference in displacements are the so called 'shear gaps'. In turn, the shear strains are determined from the interpolated shear gaps using the standard element shape functions. Compared to standard displacement formulations the method results in a modification of the shear related part of the **B**-operator matrix. DSG-elements can be classified as ANS-type or B-bar-elements.

DSG-elements have several superior properties:

1. the formulation is the same for any triangular or rectangular element,
2. the elements pass the patch test,
3. applications of the method to three-, four-, six-, and nine-node elements show that the behavior is either identical or even better than the best existing formulations available,
4. as a consequence of the nodal shear criterion, the constraint count [14] has the ideal number of 1.5, for any specific element type,
5. all necessary mathematical operations, in particular integration, are independent of the actual element shape and can be performed a priori,
6. the order of numerical stiffness integration can be reduced without activating zero energy modes; these together allow to generate an efficient element code which can be derived from existing code for displacement elements by some simple modifications of the **B**-matrices.

So far the presented formulation is restricted to linear problems. Further developments towards fully geometrically nonlinear behavior are in progress.

References

[1] Andelfinger U, Ramm E. EAS-elements for two-dimensional, three-dimensional, plate and shell structures and their equivalence to HR-elements. International Journal for Numerical Methods in Engineering 1993;36:1311–37.
[3] Bathe KJ, Brezzi F, Cho SW. The MITC7 and MITC9 plate bending elements. Computers and Structures 1989;32:797–814.
[4] Bathe KJ, Dvorkin EN. A four-node plate bending element based on Mindlin/Reissner theory and a mixed interpolation. International Journal for Numerical Methods in Engineering 1985;21:367–83.
[5] Batoz JL, Katili I. On a simple triangular Reissner/Mindlin plate element based on incompatible modes and discrete constraints. International Journal for Numerical Methods in Engineering 1992;35:1603–32.
[6] Betsch P, Gruttmann F, Stein E. A 4-node finite shell element for the implementation of general hyperelastic 3D-elasticity at finite strains. Computer Methods in Applied Mechanics and Engineering 1996;130:57–79.
[7] Bischoff M, Ramm E. Shear deformable shell elements for large strains and rotations. International Journal for Numerical Methods in Engineering 1997;40:4427–49.
[8] Bucalem ML, Bathe KJ. Higher-order MITC general shell elements. International Journal for Numerical Methods in Engineering 1993;36:3729–54.

[9] Büchter N, Ramm E. 3D-extension of nonlinear shell equations based on the enhanced assumed strain concept. In: Hirsch Ch, editor. Computational methods in applied sciences. Amsterdam: Elsevier, 1992. p. 55–62.
[10] Büchter N, Ramm E, Roehl D. Three-dimensional extension of nonlinear shell formulation based on the enhanced assumed strain concept. International Journal for Numerical Methods in Engineering 1994;37:2551–68.
[11] Fox DD, Nagtegaal JC. A unified transverse shear treatment for 3-node and 4-node stress resultant shell elements. In: The 1997 US National Conference on Computational Mechanics, San Francisco. 1997.
[12] Haußer C, Ramm E. Efficient shear deformable 3-node plate/shell elements — an almost hopeless undertaking. In: Proceedings of the Third International Conference in Computational Structures Technology CST '96, Budapest, August 21–23. 1996.
[13] Hibbit, Karlsson, and Sorensen, Inc. ABAQUS Theory Manual. 1996.
[14] Hughes TJR. The finite element method — linear static and dynamic finite element analysis. Englewood Cliffs, NJ: Prentice-Hall, 1987.
[15] Hughes TJR, Taylor RL. The linear triangular bending element. In: Whiteman JR, editor. The mathematics of finite elements and applications IV. New York: Academic Press, 1981.
[16] Hughes TJR, Tezduyar TE. Finite elements based upon Mindlin plate theory with particular reference to the four-node isoparametric element. Journal of Applied Mechanics 1981;48:587–96.
[17] Lyly M, Stenberg R, Vihinen T. A stable bilinear element for the Reissner–Mindlin plate model. Computer Methods in Applied Mechanics and Engineering 1993;110:343–57.
[18] Parisch H. A continuum-based shell theory for nonlinear applications. International Journal for Numerical Methods in Engineering 1993;38:1855–83.
[20] Pinsky PM, Jang J. A C^0-elastoplastic shell element based on assumed covariant strain interpolations. In: Pande GN, Middleton J, editors. Proceedings of the International Conference NUMETA 1987, Swansea, 1987.
[21] Ramm E, Bischoff M, Braun M. Higher order nonlinear shell formulations — a step back into three dimensions. In: Bell K, editor. From finite elements to the troll platform. Trondheim, Norway: Department of Structural Engineering, Norwegian Institute of Technology, 1994. p. 65–88.
[22] Sansour C. A theory and finite element formulation of shells at finite deformations including thickness change: circumventing the use of a rotation tensor. Archive of Applied Mechanics 1995;10:194–216.
[23] Simo JC, Rifai S. A class of mixed assumed strain methods and the method of incompatible modes. International Journal for Numerical Methods in Engineering 1990;29:1595–638.
[24] Simo JC, Armero F. Geometrically non-linear enhanced strain mixed methods and the method of incompatible modes. International Journal for Numerical Methods in Engineering 1992;33:1413–49.
[25] Szilard R. Theory and analysis of plates. Englewood Cliffs, NJ: Prentice-Hall, 1974.
[26] Simo JC, Hughes TJR. On the variational foundations of assumed strain methods. Journal of Applied Mechanics 1986;53:51–4.
[27] Xu Z. A simple and efficient triangular finite element for plate bending. Acta Mechanica Sinica 1986;2:185–92.